

Traffic Noise and the Hyperbolic Plane

G. W. Gibbons^a, C. M. Warnick^{a,b}

^a*DAMTP, CMS, Wilberforce Road, Cambridge, CB3 0WA, UK*

^b*Queens' College, Cambridge, CB3 9ET, UK*

Abstract

We consider the problem of sound propagation in a wind. We note that the rays, as in the absence of a wind, are given by Fermat's principle and show how to map them to the trajectories of a charged particle moving in a magnetic field on a curved space. For the specific case of sound propagating in a stratified atmosphere with a small wind speed we show that the corresponding particle moves in a constant magnetic field on the hyperbolic plane. In this way we give a simple 'straightedge and compass' method to estimate the intensity of sound upwind and downwind. We construct Mach envelopes for moving sources. Finally, we relate the problem to that of finding null geodesics in a squashed anti-de Sitter spacetime and discuss the $SO(3,1) \times \mathbb{R}$ symmetry of the problem from this point of view.

Keywords:

1. Introduction

In the New Scientist¹ of 15th April, 2009, a correspondent posed the following question regarding traffic noise

I live a kilometre north of a busy motorway. When the wind is coming from the south the noise of the motorway is noticeably greater than when the wind is coming from the north.

Assuming a wind speed of a mere 30 kilometres per hour, how can the wind direction affect the level of traffic noise I hear when the speed of sound is more than 1235 kilometres per hour?

This apparent paradox, and its resolution, have been known since at least the time of Stokes [1]. The explanation given by Stokes is that this effect is produced by *wind shear*, the variability in the wind speed as a function of height. This gives rise to refraction, causing

[☆]DAMTP pre-print no. DAMTP-2009-75

Email addresses: G.W.Gibbons@damtp.cam.ac.uk (G. W. Gibbons), C.M.Warnick@damtp.cam.ac.uk (C. M. Warnick)

¹issue 2704

sound rays to bend away from the ground in the upwind direction and towards the ground in the downwind direction.

As a qualitative explanation of the process, this is perfectly satisfactory, see for example the discussion of Reynolds [2]. A quantitative discussion is given by Rayleigh [3] however he assumes that the rays are normal to the wavefronts, which is not true in the presence of a wind. Rayleigh thus arrives at an incorrect equation for sound rays in a wind, as pointed out by later authors [4, 5].

Modern approaches to this problem usually involve the use of numerical ray-tracing to plot the paths of sound rays [6]. The purpose of this paper is to provide a quantitative, analytic, discussion of this effect. We consider a stratified atmosphere whose sound speed and wind speed are allowed to vary with height. Making use of geometrical ideas discussed in [7] we show that provided the wind speed is small compared to the speed of sound, and that the sound speed does not vary rapidly with height, the rays are well approximated by trajectories of a charged particle moving in a uniform magnetic field on the hyperbolic plane.

We use the equivalence between sound rays and charged particles to investigate two problems. One is that of traffic noise, outlined above. The other is the problem of the Mach envelope of a moving body in a stratified atmosphere with a small wind. We finally discuss how to lift the problem to that of finding null geodesics for a squashed anti-de Sitter spacetime, which allows us to exhibit the $SO(3, 1) \times \mathbb{R}$ symmetries in a simple fashion.

2. Fermat's principle for moving media

Consider a disturbance $u(x, t)$ obeying the wave equation

$$\left[\frac{\partial^2}{\partial t^2} - h^{ij} \frac{\partial}{\partial x^i} \frac{\partial}{\partial x^j} \right] u(x, t) = 0, \quad (2.1)$$

where $h^{ij}(x)$ is a positive definite symmetric matrix. A sound wave propagating locally in the direction n^i will have phase velocity $h_{ij}n^in^j$ at x . Here h_{ij} is the matrix inverse of h^{ij} . For the case of an isotropic fluid, we have $h^{ij} = c^2(x)\delta^{ij}$, with c the local speed of sound, but we will allow for the possibility that the speed of sound depends on the direction of propagation.

Suppose we take a disturbance whose wavelength is short compared to all other length-scales. It is well known that the energy of the wave travels along *rays* $\alpha = \alpha(\tau)$, which are extremals of the functional

$$T[\alpha] = \int \sqrt{h_{ij}\alpha^i\alpha^j} d\tau \quad (2.2)$$

Where τ is *any* parameter along the curve. We note that the integrand is simply dt , so that rays obey *Fermat's principle of least time*, i.e. a sound packet will travel from P to Q along a path which minimises² the time taken among nearby paths, subject to the condition that the packet moves always at the local speed of sound.

²strictly *extremises* – the ray may in fact maximise the time taken

Now let us consider a disturbance in a fluid with local sound speed tensor $h^{ij}(x)$ which is moving with a local velocity $W^i(x)$. This will obey a modified wave equation:

$$\left[\left(\frac{\partial}{\partial t} - W^i \frac{\partial}{\partial x^i} \right)^2 - h^{ij} \frac{\partial}{\partial x^i} \frac{\partial}{\partial x^j} \right] u(x, t) = 0. \quad (2.3)$$

What is perhaps less well known is that the sound rays in this situation also obey a form of Fermat principle: a sound packet will travel from P to Q along a path which minimises the time taken among nearby paths, subject to the condition that it moves at the local speed of sound, *relative to the flow*.

This means that a sound ray in a moving medium must solve a Zermelo navigation problem. This problem, proposed by Zermelo is to find the path between two points which minimises the time travelled, given that one moves at unit speed with respect to a ‘wind’ vector W . Taking the view that h_{ij} defines a metric, with respect to which sound moves at unit speed, the principle of least time tells us that a ray indeed solves a Zermelo problem.

The general Zermelo problem of navigation on a manifold with metric h and wind W is considered in [8]. It is shown that this problem is isomorphic with finding the Finsler geodesics of a metric in the Randers class of Finsler metrics. Randers metrics take the form

$$F : TM \setminus 0 \rightarrow \mathbb{R}^+ \\ (x, y) \mapsto \sqrt{a_{ij}(x)y^i y^j} + b_i y^i \quad (2.4)$$

Where $a_{ij}b^i b^j < 1$ is required in order that this be a good Finsler metric. The Randers metric whose geodesics solve the Zermelo problem with data (h_{ij}, W^i) is given by

$$a_{ij} = \frac{\lambda h_{ij} + W_i W_j}{\lambda^2}, \quad b_i = -\frac{W_i}{\lambda}, \quad W_i = h_{ij} W^j, \quad \lambda = 1 - h_{ij} W^i W^j. \quad (2.5)$$

The condition $a_{ij}b^i b^j < 1$ becomes $h_{ij}W^i W^j < 1$. This transformation is invertible and every Randers metric may be thought of as arising from a Zermelo problem. Geodesics of the Randers metric are (up to parameterization) the paths followed by a particle of unit charge, moving at unit speed in the magnetic field defined by $F = db$. For this reason, we will identify Randers one-forms which differ by an exact form $b \sim b + d\phi$ for most of this paper, the exception coming in Section 5 where the parameterization will be relevant.

The fact that the rays of (2.3) obey Fermat’s principle can be seen in two ways. In [9] it is shown that one may start with the Hamiltonian system following from the dispersion relation of (2.3) and show that the integral curves of the Hamiltonian obey the Euler-Lagrange equations of the time functional

$$T[\alpha] = \int \sqrt{a_{ij}\alpha^i \alpha^j} + b_i \alpha^i ds \quad (2.6)$$

with a and b defined in terms of h and W by (2.5). Since the Hamiltonian is homogeneous of degree 1 in momenta this transformation is not the standard Legendre transformation.

Alternatively, in [11] Fermat's principle is derived by considering (2.3) as the d'Alembertian operator of a 4-dimensional Lorentzian manifold. Using the fact that the rays are determined by the principal part of the wave equation (which is conformally invariant) one may derive Fermat's principle by considering the null geodesics of this Lorentzian spacetime. In [7] the relation between the Zermelo, Randers and spacetime viewpoints was explored in greater depth.

The link between magnetism and wave propagation in a moving background has also been explored in a different context by Berry et al. [10]. Here the relation is used to construct a water wave analogue for a quantum mechanical system.

3. Traffic Noise

We consider the following problem as a model for traffic noise in the vicinity of a motorway, with a stratified atmosphere such that the speed of sound varies with height above the ground and there is in addition a cross wind, also varying with height. We work in the upper half plane, with coordinates x, z and take the ground to be $z = 0$. We suppose the sound waves travel at a speed $c(z)$ and there is a horizontal wind $W = w(z)\partial/\partial x$ which vanishes at $z = 0$. Thus, we seek to solve the Zermelo problem with data

$$h = \frac{dx^2 + dz^2}{c^2(z)}, \quad W = w(z)\frac{\partial}{\partial x}. \quad (3.1)$$

The corresponding Randers data are

$$a = \frac{dx^2}{c^2(z) \left(1 - \frac{w^2(z)}{c^2(z)}\right)^2} + \frac{dz^2}{c^2(z) \left(1 - \frac{w^2(z)}{c^2(z)}\right)}, \quad b = -\frac{w(z)}{c^2(z) - w^2(z)}dx. \quad (3.2)$$

If we make the assumptions that $w(z)/c(z) \ll 1$ and $c''(z)c(z)/c'(z)^2 \ll 1$, then the Gaussian curvature of the metric a is

$$K \approx -(c'(z)^2 + 2w'(z)^2). \quad (3.3)$$

We will therefore approximate the metric a in the neighbourhood of $z = 0$ by a metric of constant negative curvature $K = -(\sigma_c^2 + 2\sigma_w^2)$, where we define for convenience $\sigma_c = c'(0)$, $\sigma_w = w'(0)$. The line $z = 0$ may be shown to have geodesic curvature

$$k_g = \sigma_c \quad (3.4)$$

so in our approximation, the surface of the ground will be a curve of constant geodesic curvature in the hyperbolic plane. σ_c is positive when the speed of sound increases with height from ground level and negative if the speed of sound decreases with height. In the model proposed, the sign of σ_c determines on which side of the curve of constant geodesic curvature the atmosphere lies.

To first order in w/c , we find

$$F = db = w'(z)\mu_a \quad (3.5)$$

where μ_a is the area form of the metric a . Thus in our approximation we will consider the sound rays to be the paths of a particle or unit charge, moving at unit speed on the hyperbolic plane with respect to a constant magnetic field σ_w .

We use these observations to map the problem to one in the hyperbolic disk³. This is the region $|\zeta| < 1$ of \mathbb{C} , endowed with the Poincaré metric

$$ds^2 = \frac{4\rho^2}{(1 - |\zeta|^2)^2} d\zeta d\bar{\zeta}. \quad (3.6)$$

This is a model of the hyperbolic plane, with constant curvature $K = -1/\rho^2$. A particle of unit charge moving in a constant magnetic field β , passing through the origin, moves along an arc of a circle of Euclidean radius

$$R_\beta = \frac{1}{2\beta\rho}. \quad (3.7)$$

Alternatively, we can characterise this arc as a curve of constant geodesic curvature β .

We will assume⁴ that the source of the noise is located at the centre of the disk. We then have the following building blocks for our geometric construction

- **Ground level** corresponds to an arc of a circle of radius

$$\frac{1}{2} \sqrt{1 + 2 \frac{\sigma_w^2}{\sigma_c^2}} \quad (3.8)$$

through the origin. If $\sigma_c > 0$, so that the speed of sound increases with height, the atmosphere corresponds to the interior of this circle otherwise it is the exterior. By a rotation we may arrange that at $z = 0$ the ground level is tangent to $\text{Im}z = 0$, with the atmosphere above the ground.

- **Sound Rays** are arcs of circles of radius

$$\frac{1}{2} \sqrt{2 + \frac{\sigma_c^2}{\sigma_w^2}} \quad (3.9)$$

passing through the origin. If $\sigma_w > 0$, so that the wind blows from left to right above ground-level, the arcs should curve to the right, else they should curve to the left.

³In a later section, we will deal with the precise mappings which take our problem over to the hyperbolic disk, but we already have sufficient information to propose a geometric construction to determine received intensity as a function of distance from the source.

⁴this is easily arranged by making use of symmetries of the Poincaré disk.

Figures 1 to 4 show sample constructions for various values of σ_c and σ_w . The ground is shaded, and rays are shown emanating from the origin at equally spaced angles of $\pi/12$. Since the Poincaré model is conformally flat, a source which radiates uniformly in all directions will radiate the same amount of energy between any two rays, $1/12$ of the total energy radiated. We assume for simplicity that there is no significant transfer of energy between the bulk fluid motion and the sound waves.

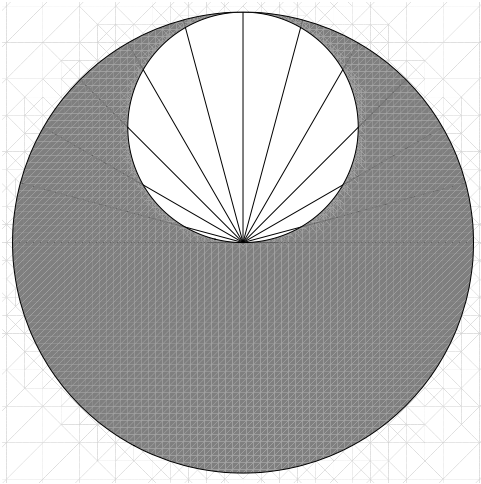


Figure 1: $\sigma_c = 1, \sigma_w = 0$

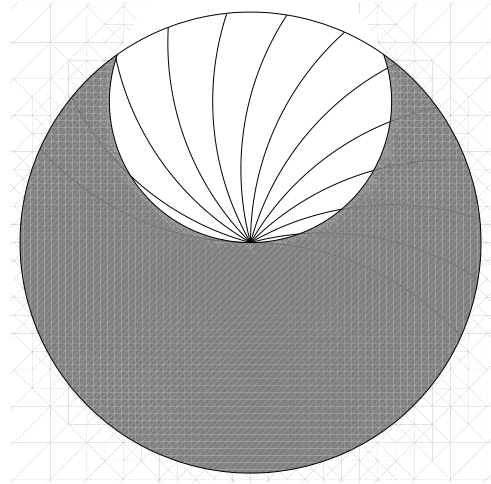


Figure 2: $\sigma_c = 1, \sigma_w = .5$

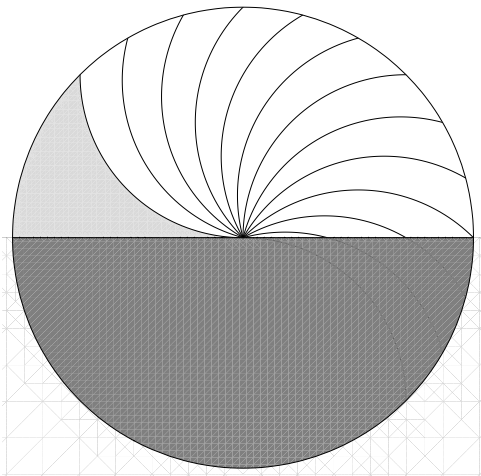


Figure 3: $\sigma_c = 0, \sigma_w = .5$

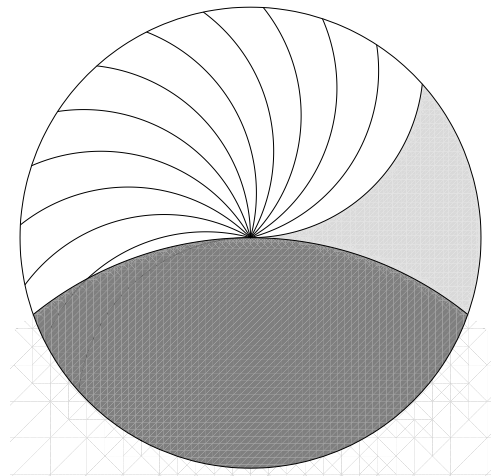


Figure 4: $\sigma_c = -1, \sigma_w = -2$

Figure 1 shows the case of vanishing wind, together with a sound speed which increases with height, such as may be caused by a ‘temperature inversion’. In this case the rays are straight lines and all return to the ground at some point. Clearly one half of the power radiated returns to each side of the source.

Figure 2 shows the case where sound speed increases with height and there is also a wind shear, with the wind blowing from left to right. In this case, not all the radiated energy returns to earth. By counting the rays, we readily estimate that roughly 5/12 of the power is lost to the atmosphere, 5/12 is received downwind (i.e. to the right) and 2/12 upwind (left) of the source.

Figure 3 shows the case where the sound speed does not vary significantly with height, but there is a wind blowing left to right. In this case, in the ray theory approximation⁵, no sound is received to the left of the source, approximately 1/4 is received to the right and the rest is radiated upwards to the atmosphere.

Figure 4 shows the case where there is a decrease in sound speed with height, together with a strong wind shear, with the wind blowing from right to left. In this case there are competing effects between the changing sound speed, which would tend to refract waves upwards and the wind shear which would tend to bend rays downwards. We see that to the right of the source there is no sound received, while roughly 1/8 of the power is received to the left. In both Figure 3 and Figure 4 there is a ‘quiet zone’, shown shaded in light grey, where no sound reaches the observer.

We see then how a simple ‘straightedge and compass’ construction allows us to make quantitative predictions about the ratio of power transmission upwind and downwind in a shearing wind. In fact, with a little more geometry it is possible to calculate, in our approximation, the intensity of sound received as a function of distance from the source. Suppose a sound ray is emitted from the source at an angle θ to the ground. It is a matter of simple circle geometry to calculate the point at which this ray again intersects the ground. Using the hyperbolic metric we can find the proper distance along the ground to this point, and we find that it is given by

$$x = c_0 \frac{\sqrt{2}}{\sigma_w} \tanh^{-1} \left(\frac{\sqrt{2} \sigma_w \sin \theta}{\sigma_w + \sigma_c \cos \theta} \right), \quad (3.10)$$

where $c_0 = c(0)$. The received intensity is then simply proportional to $\left(\frac{dx}{d\theta}\right)^{-1}$. We plot x against $\left(\frac{dx}{d\theta}\right)^{-1}$ for the same values of σ_c, σ_w as above in Figures 5 to 8.

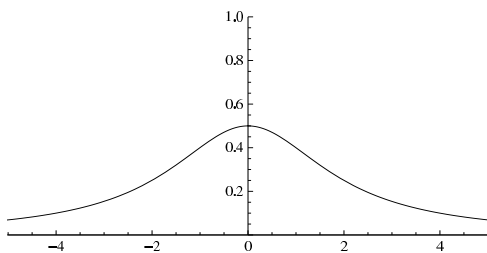


Figure 5: $\sigma_c = 1, \sigma_w = 0$

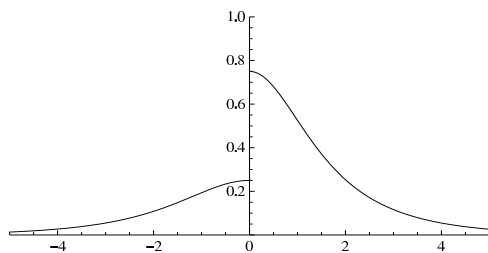


Figure 6: $\sigma_c = 1, \sigma_w = .5$

⁵We would expect that for a full solution of the wave equation the sound field will not be zero but will in fact vanish exponentially in any ‘silent’ zone of the ray theory approximation.

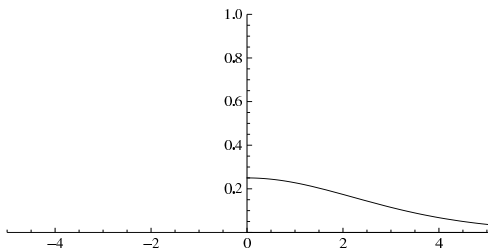


Figure 7: $\sigma_c = 0, \sigma_w = .5$

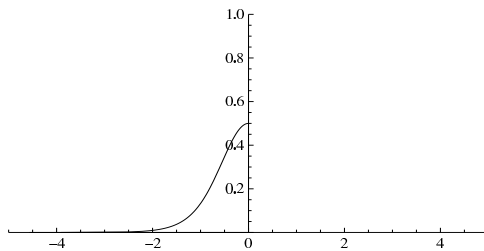


Figure 8: $\sigma_c = -1, \sigma_w = -2$

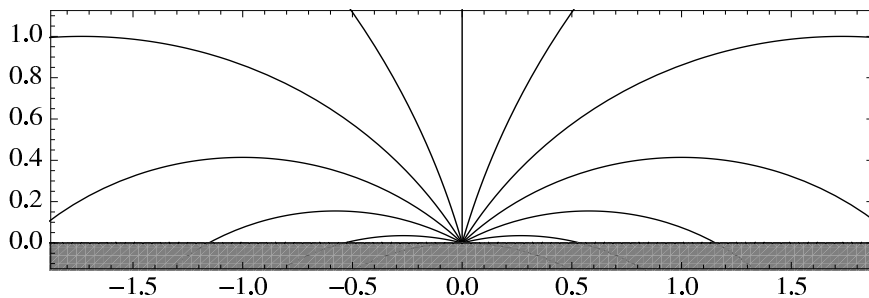


Figure 9: $\sigma_c = 1, \sigma_w = 0$

In these figures, we have set $c_0 = 1$. The vertical scale is proportional to the intensity received. The plots agree with the rough ratios we found above for the energy upwind and downwind of the source.

The approximations we have made are valid provided that $\sigma_c x/c_0$ and $\sigma_w x/c_0$ are small, so we can trust the plots in a neighbourhood of the origin. Qualitatively, we do not expect significant deviation from these plots, even outside the regime where the approximations are valid.

We note that Randers metrics and Zermelo problems are in direct, one-to-one correspondence. We might therefore choose to take the view that the preceding calculations are exact, but for an atmosphere with a slightly different sound and wind speed profile. These profiles would match the assumed shape above in a region near the ground.

4. Ray Plots

In order to plot the paths of rays in the physical x, z coordinates, we need to explicitly construct the map to a region of the hyperbolic disk, of which we have made implicit use in the preceding section. We do this in the appendix below. In this section we use the mapping to pull back the ray paths from the hyperbolic disk to the original coordinates so as to exhibit the physical paths of the rays. Figures 9 to 12 show these paths for the same parameters as the previous section.

We once again take $c_0 = 1$. We note that the ray paths are broadly as one would expect from heuristic considerations [1, 2]. In Figure 12 we explicitly see that the rays terminate at $z \approx .42$. The horizontal line here is the pull back of the conformal boundary of \mathbb{H}^2 , and the rays will take an infinitely long time to reach this height. Figures 10 and 11 would

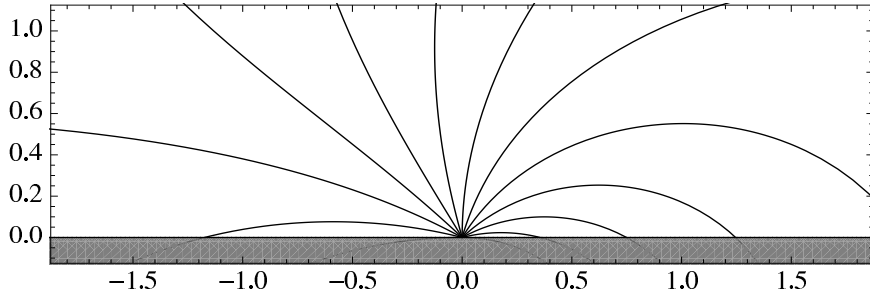


Figure 10: $\sigma_c = 1, \sigma_w = 0.5$

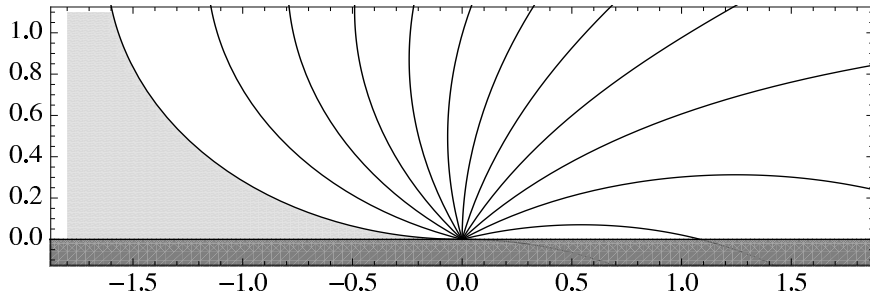


Figure 11: $\sigma_c = 0, \sigma_w = 0.5$

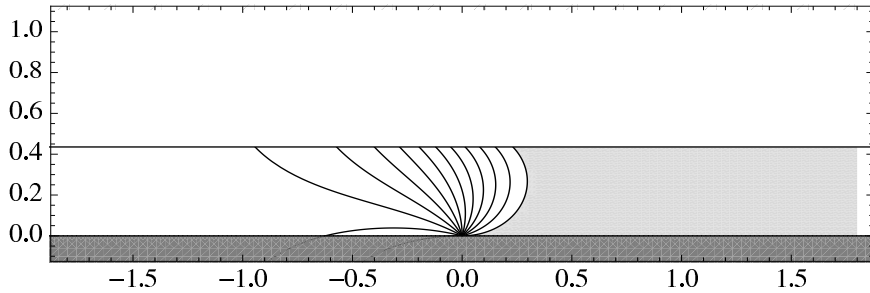


Figure 12: $\sigma_c = -1, \sigma_w = -2$

also exhibit such a phenomenon if the z -axis were extended. In practice of course, the approximations we have made are only valid in a strip about $z = 0$ and would break down before the rays reached this height.

One may verify roughly that these figures are consistent with the intensity plots given above. The energy absorbed by the ground between any adjacent rays is $\pi/12$, which should be the area under the intensity plot between the same values of x .

5. The sound field of a moving source

We now change perspective somewhat and leave behind the problem of propagation of traffic noise to instead consider a moving body which radiates sound, for example an aircraft. In the classical case of a spatially homogeneous 2-dimensional atmosphere with no wind, a subsonic aircraft moving along the z -axis at constant speed has a soundfield that fills the

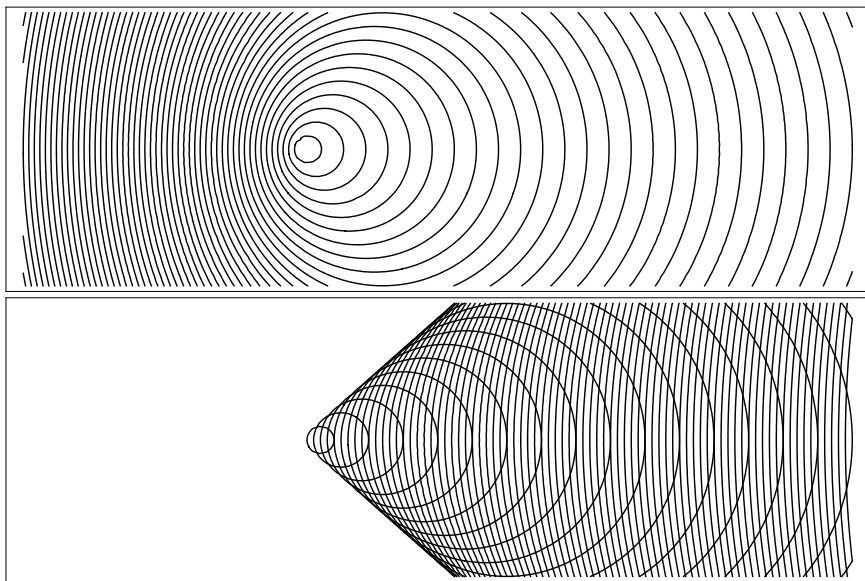


Figure 13: Example sound fields for a subsonic (t) and supersonic (b) body in a homogeneous atmosphere with no wind

whole of \mathbb{R}^2 . For an aircraft moving at a supersonic speed, the disturbances are confined inside the ‘Mach cone’ and there is a zone of silence in front of the body. There is a ‘Sonic Boom’ at the boundary of this cone. These features are shown in Figure 13. It is known that the introduction of a spatially varying sound speed gives rise to interesting, qualitatively different phenomena in the sound fields of fast moving objects [12]. We shall examine the further effects to be observed in the presence of a wind.

In order to visualise the sound field, it is convenient to imagine that the object emits pulses of sound periodically, and to plot the loci of all these disturbances at some fixed time. We work in the approximation outlined in Section 2, where the wavelength of sound is assumed to be much shorter than other lengthscales in the problem and so the disturbances propagate along geodesics of the Randers metric F of (2.4, 2.5). The locus of a disturbance emitted a time t in the past is therefore a geodesic circle of radius t with respect to the Randers metric F , centred on the point at which the disturbance originated.

We shall consider a body moving in the stratified atmosphere of Sections 3, 4 at a constant speed parallel to the x -axis. After a Galileian boost, we may assume that the wind speed is zero at the height of the body, so that it moves along $z = 0$ without loss of generality. In order to visualize the sound field as described above, we need to find the geodesic circles of the Randers metric defined by

$$a = \frac{dx^2}{c^2(z) \left(1 - \frac{w^2(z)}{c^2(z)}\right)^2} + \frac{dz^2}{c^2(z) \left(1 - \frac{w^2(z)}{c^2(z)}\right)}, \quad b = -\frac{w(z)}{c^2(z) - w^2(z)} dx, \quad (5.1)$$

centred on points of $z = 0$. Since $\partial/\partial x$ is a Killing vector of the Randers metric, we may without loss of generality consider only those geodesic circles centred on the origin.

We once again assume that $w(z)/c(z) \ll 1$ and $c''(z)c(z)/c'(z)^2 \ll 1$, so that the geodesics of the Randers metric are well approximated by the rays found in previous sections. We note that the time taken to traverse a curve $\gamma(\lambda)$ has two contributions:

$$t = \int d\lambda (\sqrt{a_{ij}\dot{\gamma}^i\dot{\gamma}^j} + b_i\dot{\gamma}^i) \quad (5.2)$$

but that (5.1) shows the $b_i\dot{\gamma}^i$ contribution to be smaller than the first contribution by a factor of w/c . We may thus approximate the length of a curve with respect to the Randers structure $a + b$ by the Riemannian length of the metric a^6 . We shall find the geodesic circles of radius t by moving a distance t , with respect to a , along the geodesics calculated in previous sections. We make use of the approximations above to map the problem to the hyperbolic disk, where the manifest rotational symmetries of the problem show that the geodesic circles we seek are in fact Euclidean circles centred on the origin. The relation between the Euclidean radius and the Randers radius is found by integrating a along an arc of a circle. Finally the transformations given explicitly in the Appendix are used to map the geodesic circle back to physical space. Combining this construction with the x -translation invariance of the physical space, we may readily plot the sound field for various values of the parameters σ_c, σ_w and for differing speeds of the radiating source, expressed as a Mach number as $v = Mc_0$, with c_0 the speed of sound at $z = 0$.

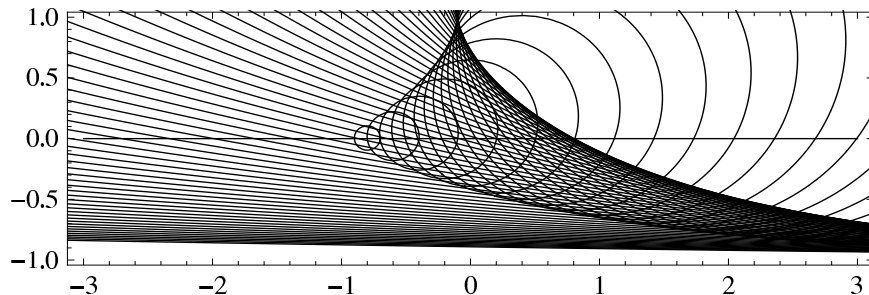


Figure 14: Sound field for a body with $M = 2$ in an atmosphere with $\sigma_c = 1, \sigma_w = 0$

Figures 14 to 16 show some sample sound fields. We see that Figure 14 is qualitatively very similar to that of [12] which considers a moving source in a stratified atmosphere whose speed of sound varies as $c(z) = (1 - z)^{-1/2}$. This particular sound speed profile is chosen so that the rays are parabolae with vertical axes. For such an atmosphere, there is no ‘zone of silence’, essentially because rays which travel into the upper half plane and are refracted back downwards can ‘overtake’ the moving source. This is because the source is moving at a speed which is supersonic only with respect to the local sound speed, whereas in this atmosphere the speed of sound increases with height so that a ray travelling at a sufficient

⁶It might seem that we have removed any possible effect the wind might have by such an assumption. It should be noted however that the geodesics themselves depend on the wind. In this approximation, we keep the *refractive* effect of wind shear, while ignoring the *transport* effect of the wind, which will be negligible for reasonable wind speeds.

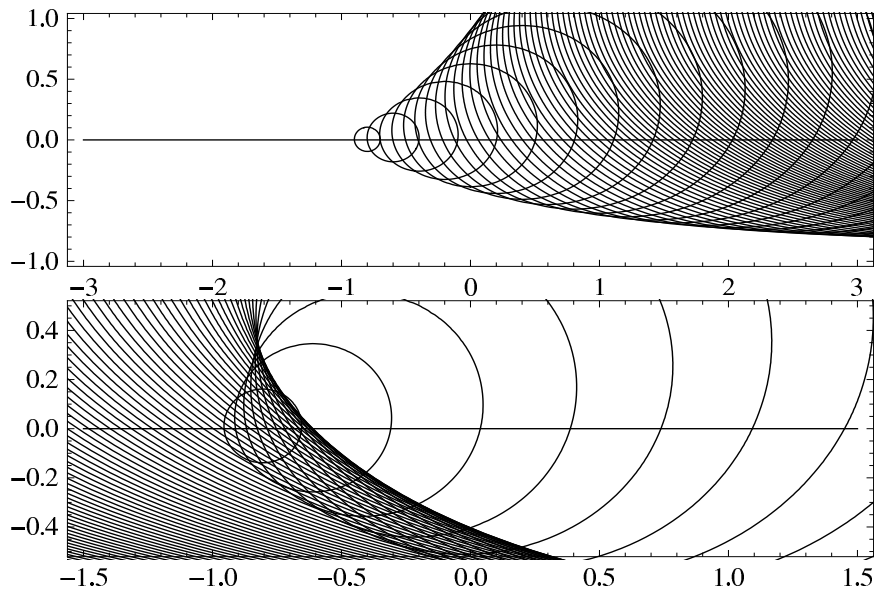


Figure 15: Sound field for a body with $M = 2$ (t) and $M = 1.3$ (b) in an atmosphere with $\sigma_c = 1$, $\sigma_w = 0.5$. Note the altered range of the lower figure.

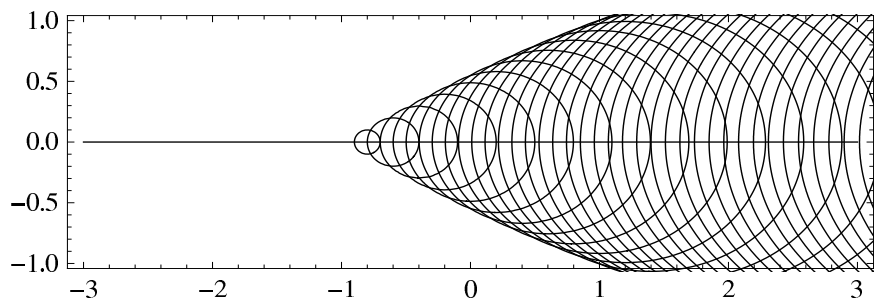


Figure 16: Sound field for a body with $M = 2$ in an atmosphere with $\sigma_c = 0$, $\sigma_w = 0.5$

height will travel faster than the source. There is however a ‘Mach envelope’, so an observer may experience a sonic boom. The envelope has a cusp at the height at which the local sound speed equals the speed of the source.

Figure 15 shows sound fields for a supersonic object moving in a stratified atmosphere with both a varying speed of sound and a wind. We find that there are two regimes. For a source moving much faster than the speed of sound, the field is similar to the Mach cone of a supersonic body in a homogeneous wind-free atmosphere, albeit distorted by the inhomogeneity. For a source which moves more slowly, but still above the local speed of sound, the picture is more similar to that of Figure 14. The reason for these different regimes is that the wind shear and varying speed of sound produce competing effects. The varying speed of sound tends to bend rays above the axis downwards, while the wind shear tends to bend rays travelling from right to left upwards. For a source travelling just over the local speed of sound, rays which travel into the upper half-plane and are refracted down may overtake the object as in Figure 14. For a source travelling considerably faster than the

local speed of sound this cannot happen as any ray which moves far enough into the upper half-plane so that it moves faster than the source is refracted by the wind shear and never returns to $z = 0$.

Figure 16 shows the case of an atmosphere whose sound speed is constant, but which has a varying wind. In this case, the sound field is similar to the Mach cone of the homogeneous wind-free case, but that the cone bends inwards slightly away from the axis due to the refraction caused by the wind shear.

6. $SL(2, \mathbb{R})$, squashed AdS_3 spacetimes and integrability

In [7] we explored a third vertex to the correspondence between the Zermelo problem and the problem of finding geodesics of a Randers metric. Both problems, and the correspondence between them, fit naturally into the problem of finding the null geodesics of a conformally stationary Lorentzian spacetime. Firstly we note that any equivalence class of metrics $[g]$ which are conformally stationary locally have a representative of the form

$$g_R = -(dt - b_i(x)dx^i)^2 + a_{ij}(x)dx^i dx^j \quad (6.1)$$

with $[g_R] = [g]$, which we call the Randers form of the metric. If we choose to parameterize the null geodesics of $[g]$ by t , then they are in fact geodesics of the Randers metric

$$F(x, y) = \sqrt{a_{ij}(x)y^i y^j} + b_i y^i \quad (6.2)$$

parameterized by unit Finslerian length. This choice of representative naturally picks out a Riemannian metric a together with a one-form b .

Another way to write a manifestly stationary spacetime, often referred to as the Painlevé-Gullstrand form, is given by

$$g_Z = -dt^2 + h_{ij}(x) (dx^i + W^i(x)dt) (dx^j + W^j(x)dt). \quad (6.3)$$

We show in [7] that $[g_Z] = [g_R]$ if and only if the Randers metric (6.2) solves the Zermelo problem with data (h_{ij}, W^i) . The condition that the Randers metric be strongly convex is also necessary to ensure that the conformal factor is nowhere singular. We thus see that the Randers and Zermelo pictures arise as different ways to write a conformally stationary class of conformal metrics.

We now have a prescription to lift the Finslerian geometry of the Randers structure to the more familiar Lorentzian geometry. The problem we have explored in depth above is that of a constant magnetic field β on the hyperbolic plane with curvature $-\kappa^2$. Following [7], we note that the lifted metric in the Randers form may be written

$$g_R = \frac{-\beta^2 (\rho^1)^2 + (\rho^2)^2 + (\rho^3)^2}{\kappa^2} \quad (6.4)$$

where the ρ_i are right invariant one-forms on $SL(2, \mathbb{R})$:

$$\begin{aligned}\rho^1 &= \frac{\kappa dt}{\beta} + \frac{1+r^2}{1-r^2} d\phi \\ \rho^2 &= \frac{2}{1-r^2} (r \cos(\kappa t/\beta) d\phi - \sin(\kappa t/\beta) dr) \\ \rho^3 &= \frac{2}{1-r^2} (r \sin(\kappa t/\beta) d\phi + \cos(\kappa t/\beta) dr).\end{aligned}\tag{6.5}$$

These arise by parameterizing $U \in SL(2, \mathbb{R})$ as

$$U = \begin{pmatrix} W+X & V-Y \\ -V-Y & W-X \end{pmatrix}, \quad \begin{aligned} X+iY &= \frac{ir}{\sqrt{1-r^2}} e^{i(\kappa t - \beta\phi)/(2\beta)}, \\ W+iV &= \frac{1}{\sqrt{1-r^2}} e^{i(\kappa t + \beta\phi)/(2\beta)}. \end{aligned}\tag{6.6}$$

The standard procedure of writing the Maurer-Cartan form

$$dUU^{-1} = \rho^i \tau_i,\tag{6.7}$$

with τ_i a basis for $sl(2, \mathbb{R})$ given in terms of the standard Pauli matrices as $\{\frac{i}{2}\sigma_2, \frac{1}{2}\sigma_3, -\frac{1}{2}\sigma_1\}$ yields (6.5).

Thus the sound rays we found are projections of null geodesics of a right-invariant metric on $SL(2, \mathbb{R})$. The ease with which we were able to construct the rays is then seen to be a consequence of symmetry. The metric (6.4) certainly admits all the left-invariant vector fields of $SL(2, \mathbb{R})$ as Killing fields. These are readily constructed as the dual basis to the left-invariant one-forms which satisfy $U^{-1}dU = \lambda^i \tau_i$ and are given by:

$$\begin{aligned}L_1 &= \frac{\partial}{\partial\phi} \\ L_2 &= \frac{1+r^2}{2r} \cos\phi \frac{\partial}{\partial\phi} + \frac{1-r^2}{2r} \left(r \sin\phi \frac{\partial}{\partial r} - \beta \cos\phi \frac{\partial}{\partial t} \right) \\ L_3 &= -\frac{1+r^2}{2r} \sin\phi \frac{\partial}{\partial\phi} + \frac{1-r^2}{2r} \left(r \cos\phi \frac{\partial}{\partial r} + \beta \sin\phi \frac{\partial}{\partial t} \right).\end{aligned}\tag{6.8}$$

In addition, since the coefficients of ρ^2, ρ^3 in the metric are the same, there is a further Killing field

$$R_1 = \beta \frac{\partial}{\partial t},\tag{6.9}$$

so that the full symmetry group of the metric is $(SL(2, \mathbb{R}) \times \mathbb{R})/\mathbb{Z}_2$. The \mathbb{Z}_2 quotient cannot be seen at the level of the Lie algebra, but one sees upon exponentiating the algebra that it is in fact a double covering of the symmetry group. Using the isomorphism

$$SO(2, 1) \cong SL(2, \mathbb{R})/\mathbb{Z}_2\tag{6.10}$$

we can also identify the symmetry group as $SO(2,1) \times \mathbb{R}$ with the $SO(2,1)$ group representing the symmetries of the hyperbolic plane and the factor \mathbb{R} the time translation symmetry. There are many similarities between the situation we are dealing with and that of right-invariant metrics on $S^3 \cong SU(2)$, which should come as no surprise since the groups are closely related by analytic continuation. The metrics we have exhibited are a natural analogue of the biaxial Berger metrics on S^3 , with symmetry group $(SU(2) \times U(1))/\mathbb{Z}_2$.

The metrics (6.4) are often referred to as describing a squashed anti-de Sitter geometry [13]. For $\beta^2 > \kappa^2$ we have a family of metrics similar to (a factor of) the Gödel universe, which include the Gödel universe⁷ as the special case $\beta^2 = 2\kappa^2$ and which all admit closed timelike curves (CTCs). For $\beta^2 < \kappa^2$ the spacetimes do not admit CTCs.

After approximation, we found above that the problem of finding sound rays for a stratified atmosphere with a wind shear is equivalent to that of finding the motion of a charge in a constant magnetic field of $\beta = \sigma_w$ in a hyperbolic space with $\kappa^2 = \sigma_c^2 + 2\sigma_w^2$, with $\sigma_c = c'(0)$, $\sigma_w = w'(0)$. Clearly we will always be in the regime where $\beta < \kappa$ so do not expect any CTCs in the lifted spacetime. This is related to the fact that any two points in the space may be joined by a Randers geodesic and these properties are explored in more detail in [7].

7. Conclusion

We have examined the old problem of ray tracing for sound waves in a wind. We find that in a certain physically plausible approximation the ray paths are mapped to the trajectories of a charged particle moving in a uniform magnetic field on the hyperbolic plane. We have exploited this fact to produce plots of the intensity of sound received from a point source at ground level in the presence of a wind and varying speed of sound. We have also constructed the approximate Mach envelopes for a moving body in the presence of a wind. We have discussed the symmetries of this model and how they relate to the problem of finding null geodesics of a family of right invariant metrics on $SL(2, \mathbb{R})$ which are often referred to as squashed AdS metrics.

Acknowledgements

GWG would like to thank Hugh Hunt for an enlightening discussion. We would also like to thank Michael Berry and John Ockendon for interesting comments on the manuscript.

Appendix - Mapping to \mathbb{H}^2 .

We start with the metric a from above:

$$a = \frac{dx^2}{c^2(z) \left(1 - \frac{w^2(z)}{c^2(z)}\right)^2} + \frac{dz^2}{c^2(z) \left(1 - \frac{w^2(z)}{c^2(z)}\right)}, \quad (.1)$$

⁷strictly speaking the Gödel universe is the product of this space with a flat direction

and make a near-identity change⁸ of the vertical coordinate

$$dy = \sqrt{1 - \frac{w^2(z)}{c^2(z)}} dz \quad (.2)$$

so that the metric may be written in the form

$$a = \frac{dx^2 + dy^2}{c^2(y) \left(1 - \frac{w^2(y)}{c^2(y)}\right)^2} = \frac{dx^2 + dy^2}{f^2(y)}. \quad (.3)$$

At this point we will explicitly approximate $f(y)$ as

$$f(y) = \alpha \cos(\beta y - \gamma) \quad (.4)$$

which for

$$\alpha = c_0 \left(1 + \frac{\sigma_c^2}{2\sigma_w^2}\right)^{\frac{1}{2}}, \quad \beta = \frac{\sigma_w}{c_0} \sqrt{2}, \quad \gamma = \sin^{-1} \left(\frac{\sigma_c}{\alpha\beta}\right) \quad (.5)$$

is accurate to $O(y^3)$. After a shift in the y coordinate defined by

$$\tilde{y} = y - \frac{\gamma}{\beta} \quad (.6)$$

we have

$$a = \frac{dx^2 + d\tilde{y}^2}{\alpha^2 \cos^2 \beta y} = \frac{d\zeta d\bar{\zeta}}{\alpha^2 \cos^2 [\beta(\zeta - \bar{\zeta})/2i]} \quad (.7)$$

where we define $\zeta = x + i\tilde{y}$. This is a (perhaps unusual) metric for the hyperbolic plane of curvature $-\alpha^2\beta^2$, where the strip $-\pi/(2\beta) < \tilde{y} < \pi/(2\beta)$ is a complete copy of the plane. We map this strip onto the standard unit disk with the conformal mapping

$$\omega = \tanh \frac{\beta\zeta}{2} \quad (.8)$$

so that the metric a becomes

$$a = \frac{4}{\alpha^2\beta^2} \frac{d\omega d\bar{\omega}}{(1 - |\omega|^2)^2} \quad (.9)$$

The ground is mapped to a curve of constant geodesic curvature passing through $\omega = \pm 1$. A final Möbius transformation leaves the metric unchanged, but shifts the ground so that it passes through the origin

$$\omega' = \frac{p\omega + i}{-i\omega + p}, \quad \text{where } p = \sqrt{2} \frac{\sigma_w}{\sigma_c} + \sqrt{1 + 2 \frac{\sigma_w^2}{\sigma_c^2}}. \quad (.10)$$

⁸in practice we may ignore this change of variables as $y = z$ to $O(y^3)$, which is the order of the approximations we make

References

- [1] G. G. Stokes, “On the Effect of Wind on the Intensity of Sound,” Report of the British Association, Dublin, 1857, p22. [Also in Mathematical and Physical Papers by George Gabriel Stokes, Vol. IV, CUP, Cambridge (1880) p110]
- [2] O. Reynolds, “On the Refraction of Sound by the Atmosphere,” Proc. Roy. Soc. **22** (1874) p531.
- [3] J. W. S. Rayleigh, “The Theory of Sound”, Macmillan (1986) §289, Vol 2.
- [4] E. A. Milne, “Sound Waves in the Atmosphere,” Phil. Mag. Series 6 (1921), **42**:247-96
- [5] E. T. Kornhauser, “Ray theory for Moving Fluids, ” Journal of the Acoustical Society of America **25** (1953) 945
- [6] M. R. Jones, E. S. Gu, and A. J. Bedard, Jr., “Infrasonic Atmospheric Propagation Studies Using a 3-D Ray Trace Model”, Proceedings, 22nd Conference on Severe Local Storms, 2004.
- [7] G. W. Gibbons, C. A. R. Herdeiro, C. M. Warnick and M. C. Werner, “Stationary Metrics and Optical Zermelo-Randers-Finsler Geometry,” Phys. Rev. D **79** (2009) 044022 [arXiv:0811.2877 [gr-qc]].
- [8] D. Bao, C. Robles and Z. Shen, “Zermelo navigation on Riemannian manifolds,” J. Diff. Geom. **66** (2004) 377-435.
- [9] R. Meyer and G. Schroeter, “The application of differential geometry to ray acoustics in inhomogeneous moving media,” Acustica **47** (1981) 105.
- [10] M. V. Berry, R. G. Chambers, M. D. Large, C. Upstill and J. C. Walmsley “Wavefront dislocations in the Aharonov-Bohm effect and its water wave analogue,” Eur.J.Phys **1** (1980), 154-162.
- [11] R. White, “Acoustic ray tracing in moving inhomogeneous fluids,” Journal of the Optical Society of America **53** (1973) 1700.
- [12] K. Kaouri, D.J. Allwright, C.J. Chapman and J.R. Ockendon, “Singularities of wavefields and sonic boom,” Wave Motion **45** (2008) 217-237.
- [13] M. Rooman and P. Spindel, “Goedel metric as a squashed anti-de Sitter geometry,” Class. Quant. Grav. **15** (1998) 3241 [arXiv:gr-qc/9804027].